

# Effect of mechanical vibration, heat treatment and ternary addition on the hysteresis in shape memory alloys

HUIBIN XU, I. MÜLLER

*FB9-Physikalische Ingenieurwissenschaften, TU Berlin, 1000 Berlin 12 FRG*

The martensitic phase transition which produces shape memory is connected with a hysteresis. Some of the applications of shape memory alloys require small hysteresis loops, other require large ones. It is therefore important to be able to control the size of the hysteresis. For that purpose three different methods were introduced in the present paper. Mechanical vibration narrowed the hysteresis loops in both NiTi and CuZnAl alloys by up to 17%, while the width of the hysteresis loops in an NiTi alloy was decreased 3 to 4 times by addition of a third element, copper. With the help of a special heat treatment a nearly hysteresis-free phase transition occurred in a Ti–51 at % Ni alloy. The size of the hysteresis is determined by the interfacial energies of the phase boundaries and these will be big, if the *E*-modulus and the lattice distortion are big.

## 1. Introduction

Shape memory alloys have in common the feature of undergoing a shear transition on cooling from the high-temperature austenitic state (A) to a low-temperature martensitic state (M) as well as on heating from M to A. These austenitic–martensitic phase transitions are hysteretic. Hysteresis loops appear in load–deformation diagrams and in deformation–temperature diagrams.

In certain commercial applications employing shape memory alloys such as in the medical field for clamps and splints [1], or for couplings [2], it is desirable that the hysteresis be wide. In other applications the hysteresis is inconvenient, because it implies dissipation. Thus in many of the proposed heat engines working with shape memory alloys [3, 4], the hysteresis loop traversed in each cycle signifies a loss.

Therefore the question arises as to how to control the size of the hysteresis. For that purpose experiments were performed in three different ways, namely mechanical vibration, heat treatment, and variation of chemical composition.

## 2. Experimental procedure

Experimental materials were Cu–26.0Zn–6.2Al (wt %), Ti–50Ni (at %), Ti–51Ni (at %) and Ti–40Ni–10Cu (at %). Ingots of Cu–Zn–Al were hot-rolled at 800 °C to sheets of 1 mm thickness. Specimens of 50 × 12.5 mm × 1.0 mm in effective size were heated at 850 °C for 1 h in an argon atmosphere and quenched in hot oil at 120 °C. Subsequently they cooled down in the quenching bath.

The TiNiCu and TiNi ingots were prepared in an induction furnace under high vacuum and annealed for homogenization. The specimens were prepared in

the same manner as the CuZnAl specimens, except that the quenching took place in ice water. The TiNiCu and Ti–50Ni specimens were also aged at 500 °C for 1 h and some Ti–51Ni specimens at 420 °C for 30 min, then quenched in ice water.

The specimens were enclosed in a heating chamber and subjected to heating–cooling cycles under a prescribed load. The resulting deformation was monitored. These tests were performed on an Instron testing machine which is capable of oscillating loads with frequencies up to 100 Hz.

## 3. Experimental results

### 3.1. Effect of mechanical vibration

A specimen of CuZnAl loaded in tension with a constant stress of 50 MPa was heated and cooled by a cycling liquid. After several temperature cycles we obtained a regular deformation–temperature curve which is shown in Fig. 1 by the outer hysteresis loop.

The specimen was then subjected to a load vibration of amplitude 10 MPa around the mean value 50 MPa at 30 Hz. After this “training” the deformation–temperature diagram exhibited a smaller hysteresis as shown by the inner curve in Fig. 1. The width of the hysteresis had decreased from 13 to 11 °C, i.e. by about 15%.

A similar experiment was also conducted with the Ti–50Ni specimens under a load vibration of amplitude 10 MPa around 40 MPa at 30 Hz. In this case the width of the hysteresis decreased from 40 to 33 °C, i.e. by about 17%, as shown in Fig. 2.

Other attempts with different, even higher frequencies were not effective; they did not lead to a further decrease of the width of the hysteresis. This research continues. We are planning to apply a wider range of

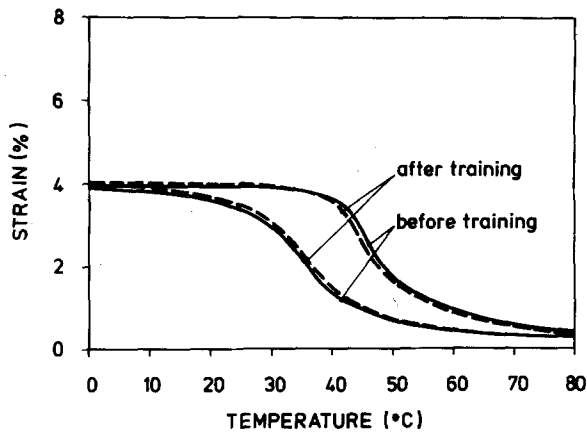


Figure 1 Effect of mechanical vibration on the hysteresis in CuZnAl.

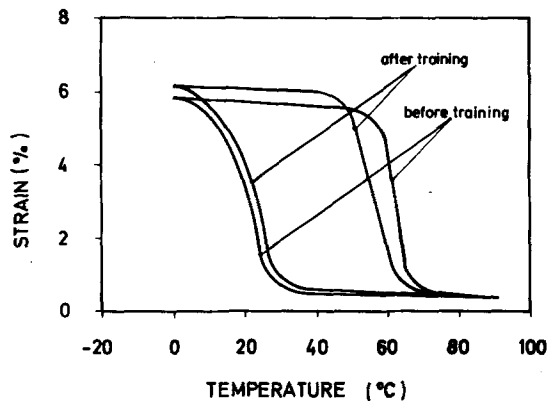


Figure 2 Effect of mechanical vibration on the hysteresis in Ti-50Ni.

stitution of  $\text{CuO}(\text{Cu}_2\text{O})$  in the eutectic melt. The substitution of antimony for tin is evidenced by the variation of the lattice parameters of  $\text{SnO}_2$  shown in Fig. 2 and Table VI.

The determined values for the linear shrinkage and porosity evidence a high densification of samples,

### 3.2. A phase transition with extremely small hysteresis in NiTi

A Ti-51Ni specimen prepared as described in Section 2 but without ageing exhibits the deformation-temperature hysteresis at 40 MPa shown in Fig. 3. The approximate width is 40°C and the loop lies at low temperatures.

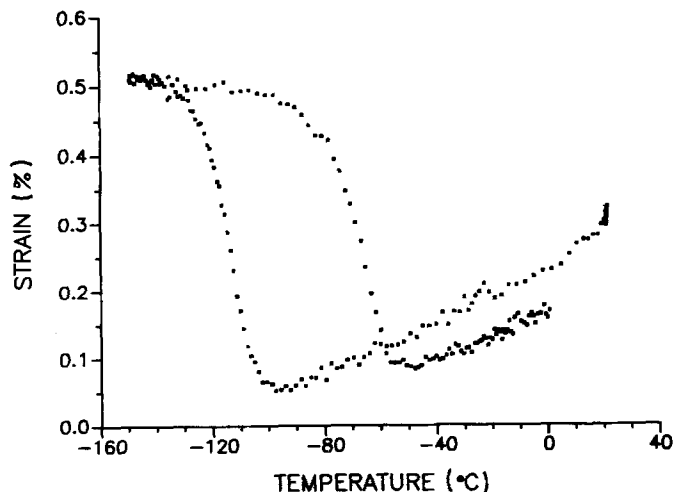


Figure 3 Hysteresis loop in Ti-51Ni at a tensile stress of 40 MPa.

The same specimen aged at 420°C for 30 min and quenched in ice water shows a quite different behaviour (Fig. 4). Apparently, the transformation now proceeds in two steps both in heating and cooling, because there are two steps in the heating and cooling curves shown in Fig. 4a. The high-temperature step is usually associated with the formation of an R-phase. We note that this step is practically reversible, i.e. it assumes nearly the same deformations upon heating and cooling. This fact is emphasized by the curves in Fig. 4b. This plot was obtained by stopping the cooling process at progressively higher temperatures so that eventually only the reversible R formation is left. Thus a deformation-temperature diagram appears with approximately 0.6% strain and an extremely small hysteresis of 1 to 2°C.

Fig. 5 shows the same phenomenon at a higher load. In this case the reversible strain of the R-phase is about 0.8%.

### 3.3. The hysteresis of TiNiCu

The deformation-temperature diagrams of a TiNiCu specimen prepared as described in the previous section are very distinct hysteresis loops as shown in Fig. 6. The widths of the hysteresis loops for different loads are nearly the same and are 9°C, which is much smaller than that of NiTi (except the R-phase) and even smaller than that of CuZnAl. However, the yield point of TiNiCu alloy is quite low and a plastic deformation appears already at 100 MPa as seen in Fig. 6b. Subsequent cycles at 100 MPa exhibit similar hysteresis loops like Fig. 6b, but the additional plastic deformation decreases (Fig. 6c). Comparing the mechanical properties of NiTi and TiNiCu alloys, we obtained the following data: the yield point to plastic deformation of TiNiCu is about 1/3 of that the NiTi, while the  $E$ -modulus of TiNiCu is 60% of that of NiTi, namely  $32 \text{ kN mm}^{-2}$  for NiTi and  $20 \text{ kN mm}^{-2}$  for TiNiCu.

## 4. Discussion

### 4.1. Effect of mechanical vibration

Inspection of Figs 1 and 2 shows that the "training" of the specimen by an oscillatory force has made both transitions  $M \rightarrow A$  and  $A \rightarrow M$  easier. This must be

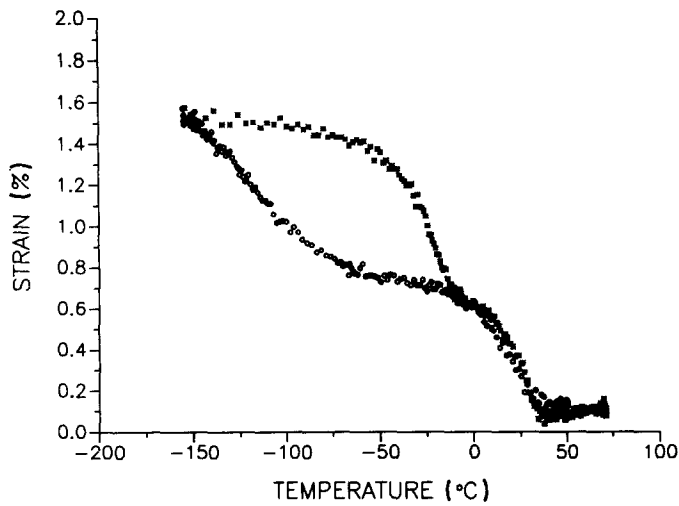


Figure 4 (a, b) Deformation-temperature diagrams of an aged Ti-51Ni specimen at a tensile stress of 40 MPa: (○) cooling, (■) heating.

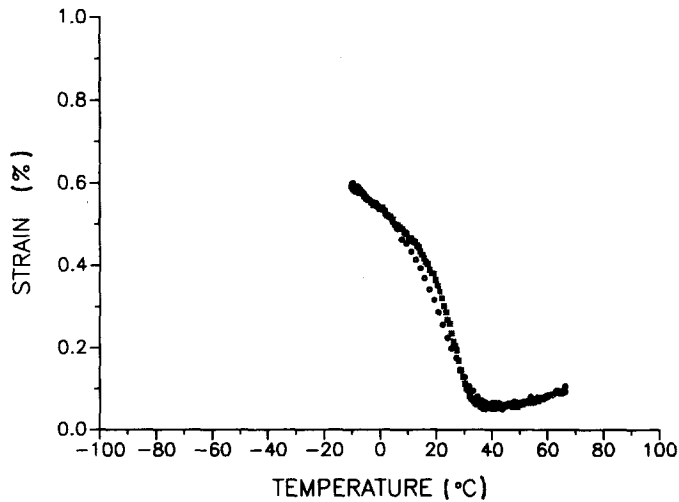
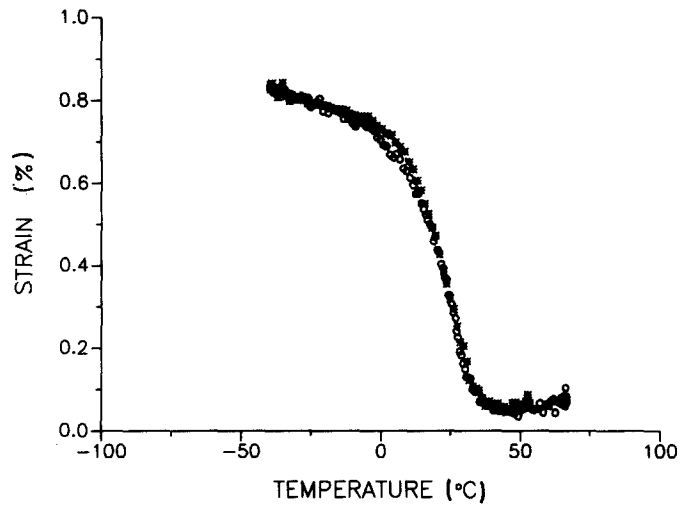


Figure 5 Deformation-temperature diagram of an aged Ti-51Ni specimen at a tensile stress of 80 MPa: (○) cooling, (■) heating.



due to an effective decrease by the oscillation of the energetic barriers that separate the positions of the austenitic and martensitic layers. The exact nature of this training phenomenon is as yet unknown.

#### 4.2. Reversible transition of R-phase

The formation of two steps in the phase change of Figs 4 and 5 is often interpreted as due to the formation of a "pre-martensitic" so-called R-phase [5]. The structure of the R-phase may exhibit but little distortion from the austenitic phase, which has a  $B_2$  structure of which CsCl is the prototype.

Figs 7 and 8 show the lattice structures relevant here. Figs 7a and b present some lattice cells of austenite. The solid lines in Fig. 7b identify a tetragonal unit cell having  $b = c = 0.427$  nm and  $a = 0.302$  nm. In Fig. 8 we have shown the monoclinic cell that emerges from the tetragonal cell of Fig. 7b in an  $A \rightarrow M$  transition. This monoclinic cell has been sheared in the direction  $\langle 110 \rangle_A$  with a shear system of  $\{100\}_A$  and  $\langle 110 \rangle_A$ . The martensitic cell has nearly the same volume ( $V$ ) as the austenitic one.

The R-phase lattice is very close to the A lattice, as can be seen from an inspection of Table I which has been taken from the literature.

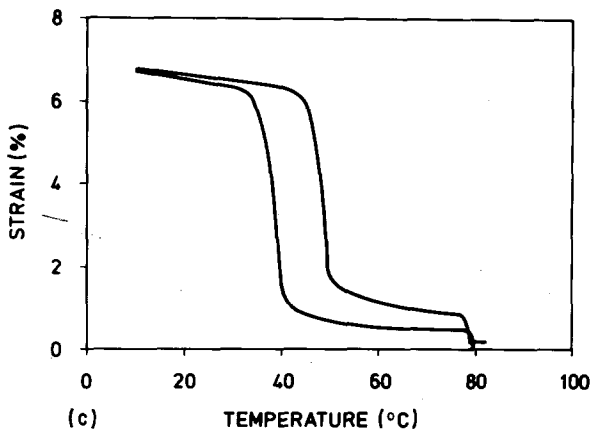
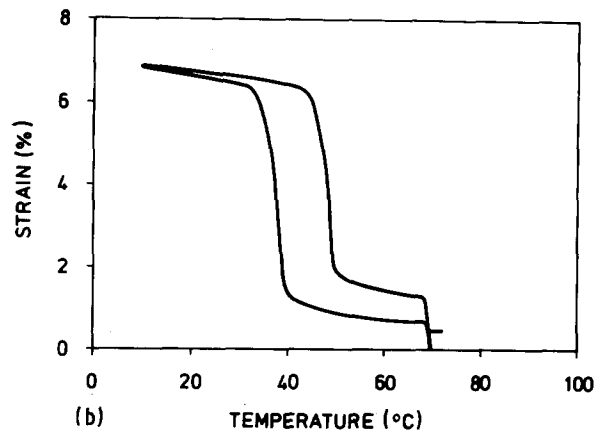
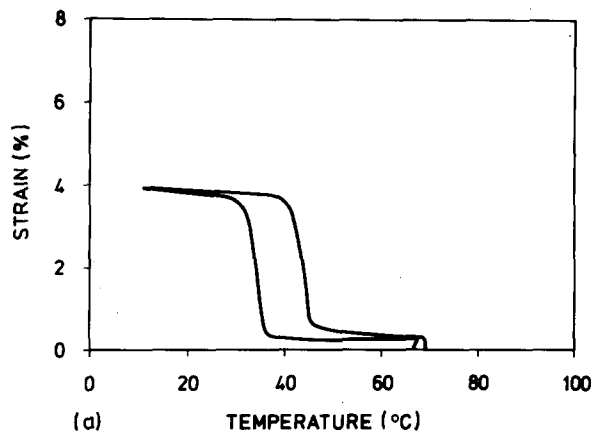


Figure 6 Hysteresis loops in TiNiCu at (a) 50 MPa, (b) 100 MPa, (c) 100 MPa.

The closeness reveals itself if we look at the  $d$ -spacings which are nearly identical for the planes  $(100)_A$ ,  $(11.1)_R$ ;  $(110)_A$ ,  $(03.0)_R$ ; and  $(111)_A$ ,  $(00.3)_R$ . This fact confirms the view that the lattice cell of the R-phase is rhombohedrically distorted by a very small amount from the A-phase (see Fig. 9).

The appearance of the R-phase may be due to precipitates of  $Ti_3Ni_4$  generated in the ageing process.

These precipitates are rich in nickel and that leaves the matrix poor in nickel. In this case it is known that an additional step is introduced into the transition  $B_2 \rightleftharpoons$  monoclinic, so that they become transitions  $B_2 \rightleftharpoons$  rhombohedral  $\rightleftharpoons$  monoclinic. Kainuma *et al.* [7] have observed the microstructure of the rhombohedral R-phase containing  $Ti_3Ni_4$  precipitates. From their results it may be inferred that the strain field caused by the precipitates causes the R-phase, because there is a very small difference of the  $d$ -spacings between the R-phase and the  $Ti_3Ni_4$  precipitates (see Table I).

We have seen that the transition  $A \rightleftharpoons R$  is scarcely hysteretic, while the transition  $R \rightleftharpoons M$  has a strong hysteresis. On the other hand, from Table I we have concluded that the  $A \rightleftharpoons R$  transition produces only a tiny deformation of the lattice, while the  $R \rightleftharpoons M$  transition involves a big shift of the lattice. These two observations may well be connected. Indeed, according to Müller [8], the size of the hysteresis is deter-

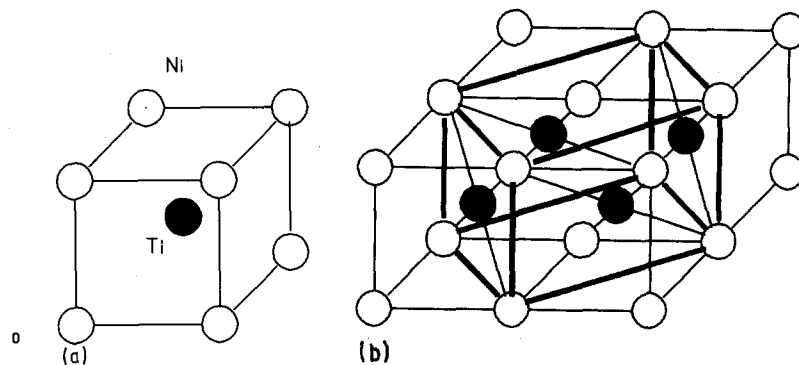


Figure 7 (a) Austenite unit cell with  $B_2$  structure ( $a = b = c = 0.3015$  nm,  $\beta = 90$ , deg. =  $100^\circ$ ,  $V = 0.02741$  nm<sup>3</sup>). (b) Four  $B_2$  unit cells and one tetragonal unit cell.

TABLE I Comparison of  $d$ -spacings of four phases [6].

A( $B_2$ )		$Ti_3Ni_4$		R		M	
( $hkl$ )	$d$ (nm)	( $hkl$ )	$d$ (nm)	( $hkl$ )	$d$ (nm)	( $hkl$ )	$d$ (nm)
100	0.302	210	0.298	11.1	0.302	100	0.289
110	0.213	321	0.213	03.0	0.212	020	0.206
111	0.174	111	0.169	00.3	0.176	101	0.191

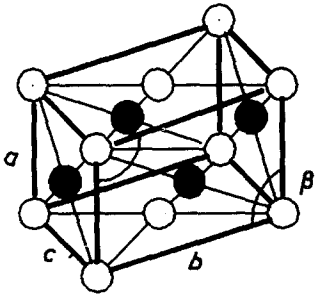


Figure 8 Unit cell of martensitic phase. For M:  $a = 0.2898$  nm,  $b = 0.4646$  nm,  $c = 0.4108$  nm,  $\beta = 96.8$  deg.,  $V = 0.05479$  nm<sup>3</sup>. For A:  $a = 0.3015$  nm,  $b = 0.4263$  nm,  $c = 0.4263$  nm,  $\beta = 90$  deg.,  $V = 0.05478$  nm<sup>3</sup>.

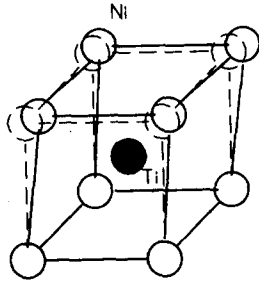


Figure 9 R-phase unit cell sheared from A.

mined by the interfacial energies of the phase boundaries and these will be big, if the lattice distortion is big. On that count we do not expect a big hysteresis in the  $A \rightleftharpoons R$  transition.

#### 4.3. The influence of copper on NiTi

The addition of a third element, copper, decreases the size of the hysteresis which is determined by the

interfacial energy. This energy  $e$  is again determined by the degree of lattice distortion ( $\Delta\varepsilon$ ) and the  $E$ -modulus, i.e.  $e = f(\Delta\varepsilon, E)$ .  $e$  will increase with  $\Delta\varepsilon$  and  $E$ . The lattice distortion of TiNiCu should be nearly the same as that of NiTi, because the only difference is the substitution of part of the Ni-atoms by copper atoms, while the  $E$ -modulus of TiNiCu is about 60% of that of NiTi. Thus, we can conclude that the small hysteresis of TiNiCu originates from the small interfacial energy due to the low value of  $E$ -modulus.

In this way we can understand qualitatively that CuZnAl alloys have small, CuAlNi bigger and NiTi large hystereses, since we know that the first has a small, the second a bigger and the last a large  $E$ -modulus. Of course, the lattice distortion, which is to be measured, also plays an important role.

#### References

1. G. BENSMANN, F. BAUMGART und J. HARTWIG, *Tech. Mitt. Krupp, Forsch. Ber.* **37** (1979).
2. D. STÖCKEL, *Metall* **41** (1987) 494.
3. R. BANKS, in Proceedings, "Shape Memory Effects in Alloys", edited by J. Perkins (Plenum, 1975) p. 537.
4. D. M. GOLDSTEIN and L. J. McNAMARA (eds.) Proceedings of the Nitinol Heat Engine Conference, September 1978, Silver Spring, Maryland.
5. C. M. WAYMAN, in Proceedings of International Symposium on Shape Memory Alloys, edited by Y. Chu, T. Y. Hsu and T. Ko, Guilin, China, 1986, p. 59.
6. T. HONMA, *ibid.* p. 83.
7. R. KAINIMA, M. MATSUMOTO and T. HONMA, in Proceedings of International Conference of Martens, Trans. ICOMAT-86 (Japan Institute of Metals, Nara, Japan, 1986) p. 717.
8. I. MÜLLER, *Continuum Mech. Thermodyn.* **1** (1989) 125.

Received 5 February

and accepted 19 February 1990